



OPEN ACCESS

EDITED BY

Chixin Xiao,
University of Wollongong, Australia

REVIEWED BY

Linfei Yin,
Guangxi University, China
Nishant Kumar,
Indian Institute of Technology Jodhpur, India

*CORRESPONDENCE

Nan Zhu,
✉ 67742123@qq.com

RECEIVED 07 February 2024

ACCEPTED 08 April 2024

PUBLISHED 03 May 2024

CITATION

Zhu N, Ma X, Guo Z, Shen C and Liu J (2024),
Research on the optimal capacity configuration
of green storage microgrid based on the
improved sparrow search algorithm.
Front. Energy Res. 12:1383332.
doi: 10.3389/fenrg.2024.1383332

COPYRIGHT

© 2024 Zhu, Ma, Guo, Shen and Liu. This is an
open-access article distributed under the terms
of the [Creative Commons Attribution License
\(CC BY\)](#). The use, distribution or reproduction in
other forums is permitted, provided the original
author(s) and the copyright owner(s) are
credited and that the original publication in this
journal is cited, in accordance with accepted
academic practice. No use, distribution or
reproduction is permitted which does not
comply with these terms.

Research on the optimal capacity configuration of green storage microgrid based on the improved sparrow search algorithm

Nan Zhu^{1,2*}, Xiaoning Ma^{1,2}, Ziyao Guo^{1,2}, Chen Shen^{1,2} and Jie Liu³

¹State Grid Liaoning Electric Power Supply Co., Ltd. Branch Materials, Shenyang, China, ²State Grid Corporation of China, Beijing, China, ³School of Electrical Engineering, Shenyang University of Technology, Shenyang, China

Green storage plays a key role in modern logistics and is committed to minimizing the environmental impact. To promote the transformation of traditional storage to green storage, research on the capacity allocation of wind-solar-storage microgrids for green storage is proposed. Firstly, this paper proposes a microgrid capacity configuration model, and secondly takes the shortest payback period as the objective function, and uses the improved sparrow search algorithm (ISSA) for optimization. Firstly, the Logistic-Tent compound chaotic mapping method is added to the population initialization of the sparrow search algorithm (SSA). Secondly, the adaptive t-distribution mutation is used to improve the discoverer, and the overall optimization ability of the algorithm is improved. Finally, the hybrid decreasing strategy is adopted in the process of vigilance position update. The ISSA can improve the search efficiency of the algorithm, avoid premature convergence and enhance the robustness of the algorithm, which is helpful to better apply to the optimal configuration of wind-solar-storage microgrid capacity in green storage. By analyzing the optimal capacity allocation results of two typical days, the system can better adapt to the dynamic storage requirements and improve the flexibility and sustainability of the supply chain.

KEYWORDS

green storage, microgrid, capacity configuration, wind-solar-storage system, sparrow search algorithm

1 Introduction

With the growing global concern for environmental sustainability, green storage, as an important component of modern logistics systems, has attracted extensive research interest (Jiang, 2021). In traditional storage systems, the high dependence on energy and the increase in environmental load has become a problem that cannot be ignored (Ma, 2023). Green energy and energy structure transformation are important changes in the current and future development of logistics parks. Rational use of clean energy is the key to achieving carbon neutrality (Liu, 2023). Therefore, researchers have turned to the search for more environmentally friendly and efficient storage solutions, among which wind-solar-storage systems have attracted much attention as a potential green energy solution (Li et al., 2023).

As the main renewable energy, wind energy and solar energy have been widely used and studied in various fields (Lazaroiu et al., 2023; Xu et al., 2024). In the logistics park, the use of

the wind-solar-storage system can effectively deal with the instability and security problems that may be brought to the power system when renewable energy is introduced (Saxena et al., 2021; Jiang J. et al., 2023). This system not only helps to improve the stability of the power system, but also significantly reduces the energy consumption and carbon emissions of the logistics park, to achieve the goal of sustainable development (Kumar et al., 2019; You, 2024). With the dynamic change in storage demand, how to accurately and efficiently configure the capacity of wind and solar energy storage systems in the change has become an urgent problem to be solved (Li et al., 2016; Dulău, 2023). At present, there are few studies on the optimal allocation of wind-solar-storage capacity for green storage at home and abroad, but most of the optimal allocation of wind-solar-storage capacity is distributed in demand response and energy management (Nan, 2023).

Demand response plays an important role in optimizing the capacity configuration of wind-solar-storage system. Through the reasonable introduction and implementation of a demand response mechanism, the efficient, stable and sustainable operation of the power system can be realized, and the wide application and development of clean energy can be promoted (Chen, 2023a). In the problem of demand response, Jiang Z. et al. (2023) considered several demand response mechanisms with flexible load participation and established an energy storage economic configuration model, which effectively reduced system costs and improved energy consumption. Guo et al. (2022) added the electric vehicle model to the microgrid model based on the time-of-use electricity price and made full use of the flexible charging and discharging characteristics of electric vehicles to configure the capacity of the microgrid. Lei et al. (2024) proposed a two-layer optimal configuration method of microgrid based on stepped carbon trading and price-based demand response. Through two-layer optimization, the impact of carbon trading and demand response on system performance is fully considered, to realize the comprehensive optimization of microgrid system. The above literature covers several studies in the field of demand response, aiming to improve the economy and efficiency of the system by optimizing the capacity of different energy systems, and to promote the consumption level of renewable energy.

However, in the face of increasing energy demand and environmental protection pressure, effective energy management can not only improve energy efficiency but also achieve stable and sustainable development of system operation (Yan, 2024). Kumar et al. (2020) proposed a novel adaptive control technology AM-MKF (Adaptive Maximise-M Kalman Filter) and a novel MPPT technology L-HC (Learning-based Hill Climbing) for solar PV grid integrated system, to alleviate the oscillation problem of the system under steady-state conditions and improve the response speed of the system to dynamic changes. In the problem of energy management, Wu et al. (2023) optimized the configuration of the wind-solar power generation coupled hydrogen energy storage model from the aspects of economic and social benefits, which not only realized the efficient utilization of energy resources but also took into account the impact and benefits on society. Xu et al. (2024) not only considered the economy and reliability of the system, but also considered the environmental benefits. By introducing the carbon trading mechanism, the carbon emission reduction capacity of the

microgrid was improved. In order to improve the economic and environmental benefits of microgrid systems, Wang et al. (2023) established the carbon emission measurement and carbon trading mechanism of microgrid systems, and effectively improved the economy of microgrid systems on the premise of reducing carbon emissions as much as possible. The above research aims to improve system reliability, improve the utilization efficiency of clean energy reduce energy consumption costs, and take into account the impact on the environment and society.

Aiming at the research of microgrid capacity optimization configuration algorithm, swarm intelligence algorithm has been widely used. Wang et al. (2022) used the particle swarm optimization algorithm to solve the model, but the algorithm is easy to fall into the local optimal solution. Zhao et al. (2022) adopted the improved grey wolf optimization algorithm. By combining a variety of improvement strategies, the problem that the grey wolf optimization algorithm is easy to fall into local optimum is improved. Yang (2010) adopts the bat algorithm and compares the improved particle swarm optimization algorithm with the genetic algorithm. However, the bat algorithm has some defects in the process of solution exploration, that is, the lack of an effective mutation mechanism, which leads to a certain probability of bat individuals falling into the local optimal solution. To solve the problem that the algorithm is easy to falls into the local optimal solution and the convergence accuracy is insufficient when dealing with the non-zero solution objective function, this paper proposes an improved sparrow search algorithm.

In summary, based on the consideration of time-of-use electricity price, this paper optimizes the capacity configuration model of microgrid systems for green storage. The improved sparrow search algorithm (ISSA) is used to optimize the microgrid capacity configuration model, including the introduction of a Logistic-Tent composite chaotic mapping strategy, adaptive t-distribution variation strategy, and mixed decreasing strategy. Two typical days are selected to solve the model to verify the effectiveness of the proposed model and the improved algorithm.

2 Microgrid capacity optimization configuration model for green storage

2.1 Structure and model of wind-solar-storage system

2.1.1 Wind-solar-storage system structure

Yang et al. (2023) proposed that the core concept of green storage is to realize the recycling of resources and energy inside and outside the storage system by imitating the operation principle of the natural ecosystem, to achieve the economic, efficient, and environmentally friendly operation objectives. In the configuration of the wind-solar-storage system, the generation of electric energy and the satisfaction of the storage power demand are regarded as part of the internal cycle. At the same time, selling excess electricity back to the power grid and interacting with the power grid constitutes another part of the external cycle. These two aspects work together to build a comprehensive application of wind-solar-storage in the green storage system. The structure of the wind-solar-storage microgrid system proposed in this paper is shown in Figure 1.

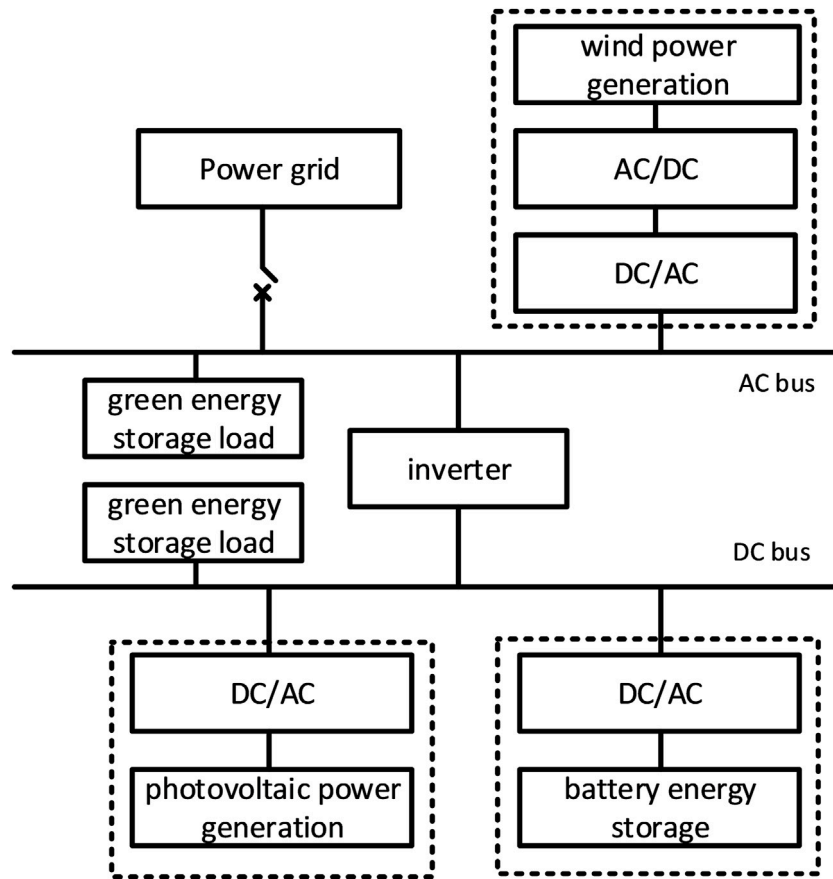


FIGURE 1 Green storage of wind-solar-storage microgrid system structure.

2.1.2 Photovoltaic power generation output model

In this paper, the photovoltaic power (PV) generation model proposed by Gao et al. (2023) and Diaf et al. (2007) is adopted. The output power of the PV generation system of this model can be calculated by Eq. 1.

$$P_{pv} = N_{pv} \times P_{e-pv} \times \frac{S}{S_{ref}} [1 + K_t(T_c - T_{ref})] \quad (1)$$

Where P_{e-pv} is the rated output power of the PV array at the working point; S_{ref} is the solar irradiance under standard conditions; S is the actual solar irradiance at the working point; K_t is the power temperature coefficient; T_c is the temperature at the working point; T_{ref} is the temperature under standard conditions; N_{pv} is the number of PV array units.

2.1.3 Wind power generation output model

In this paper, the wind power generation output model proposed by Justus (1978) and Borhanazad et al. (2014), and Su et al. (2023) is adopted. The output power of the wind turbine (WT) of this model can be calculated by Eq. 2.

$$P_{wt} = \begin{cases} 0, & V \leq V_{in}, V \geq V_{out} \\ N_{wt} (V^3 a - P_e b), & V_{in} < V < V_e \\ N_{wt} P_e, & V_e < V < V_{out} \end{cases} \quad (2)$$

Where P_{wt} is the output power of the WTGs; N_{wt} is the number of wind turbine generator systems (WTGs); P_e is the rated power of the WTGs; V is the actual wind speed; V_{in} is the cut-in wind speed; V_{out} is the cut-out wind speed; V_e is the rated wind speed. Where a and b are computed as follows.

$$a = \frac{P_e}{V_e^3 - V_{in}^3}, b = \frac{V_{in}^3}{V_e^3 - V_{in}^3} \quad (3)$$

Where P_e is the rated power of the WTGs; V_{in} is the cut-in wind speed; V_e is the rated wind speed.

2.1.4 Energy storage system model

Considering the advantages of mature battery energy storage technology, fast response speed, and relatively low price, this paper chooses centralized battery energy storage as the focus of research to optimize the capacity of wind-solar-storage microgrid systems.

The mathematical energy model of the battery in the state of charge is:

$$E_{bat} = E_{bat}(t-1)(1-\delta) + P_c(t-1)\eta_c \Delta t \quad (4)$$

The mathematical energy model of the battery in the discharged state is:

$$E_{bat} = E_{bat}(t-1)(1-\delta) + \frac{P_d(t-1)}{\eta_d} \Delta t \quad (5)$$

Where E_{bat} is the power stored in the battery at the time of t ; P_c and P_d are the charging and discharging power respectively; δ is the loss rate of the battery discharge; η_c and η_d are the charging and discharging efficiency respectively; Δt is the sampling circumference.

2.2 Optimization objective function and constraints

2.2.1 Objective function

In this paper, considering the economy, reliability, and environmental protection of the system, the shortest payback period is taken as the objective function, and the Equation is shown below:

$$\min C = \frac{C_{out} - I_{SUB}}{C_{in} + I_R - C_m} \quad (6)$$

Where C_{out} is the investment cost of WT, PV, and batteries; I_{SUB} is the government subsidy; C_{in} is the income from the sale of electricity from PV and WT; I_R is the recovery income from the system; C_m is the operation and maintenance cost of the wind-solar-storage system.

(1) Investment costs

$$C_{out} = C_{ins} \frac{r_s(1+r_s)^n}{(1+r_s)^n - 1} \quad (7)$$

Where C_{ins} is the total capital cost of the system; r_s is the discount rate; n is the useful life of the equipment.

(2) Government subsidies

$$I_{SUB} = E \times x_{sub} \times \sum_{i=0}^N \frac{1}{(1+r_s)^i} \quad (8)$$

Where E is the annual generation of WT and PV system, kWh; x_{sub} is the subsidy per kWh of WT and PV power generation, yuan/kWh, and the subsidy per kWh of power generation used in this paper is 0.45 yuan.

(3) Revenue from electricity sales

The system sells the excess electricity generated by the PV and the WT, and the revenue earned is the revenue from the sale of electricity, which is expressed as:

$$C_{in} = p_{in} \left[\sum_{t=1}^{8760} N_{pv} P_{pv}(t) + N_{wt} P_{wt}(t) \right] \Delta t \quad (9)$$

Where p_{in} is the selling price of electricity, Yuan/kWh.

(4) Recovery of benefits

$$I_R = \frac{x_R \times S}{(1+r_s)^N} \quad (10)$$

Where x_R is the unit area of the WT or PV panel recycling price, yuan/m². At present, China's energy storage battery recycling industry has not been formed, and its recycling value has not yet been available for reference data, which is not considered in this paper for the time being.

(5) Operation and maintenance costs

During the operation of the system, regular maintenance and management of the power generation units is required to ensure that the PV panels, WTGs, and batteries can operate in a stable and normal manner. The cost incurred by these maintenance activities is known as the maintenance cost, expressed as:

$$C_m = \left[\sum_{t=1}^{8760} N_{PV} C_{PVu} P_{PV}(t) + N_{WT} C_{WTu} P_{WT}(t) + N_{LB} C_{LBu} P_{LB}(t) \right] \Delta t \quad (11)$$

Where C_m are the annual operation and maintenance costs of the system; N_{PV} , N_{WT} , N_{LB} represent the number of PV panels, WTGs and batteries, respectively; C_{PVu} , C_{WTu} and C_{LBu} are the maintenance cost per unit capacity of PV panels, WTGs, and batteries respectively; $P_{PV}(t)$, $P_{WT}(t)$, $P_{BS}(t)$ are the output power of PV, WT and battery at time t , respectively.

2.2.2 Constraints

(1) System power balance constraints

Setting the limiting conditions for the output power of the wind-solar-storage microgrid systems at any moment is shown in the following Equation:

$$P_{WT}(t) + P_{PV}(t) + P_{BS}(t) \geq P_{LOAD}(t) \quad (12)$$

Where $P_{PV}(t)$, $P_{WT}(t)$, $P_{BS}(t)$ are the output power of PV, WT and battery at time t , respectively; $P_{LOAD}(t)$ is the load power.

(2) Battery storage charging and discharging power, depth of discharge

$$S_{min} \leq S(t) \leq S_{max} \quad (13)$$

$$\begin{cases} P_{c, min} \leq P_c \leq P_{c, max} \\ P_{d, min} \leq P_d \leq P_{d, max} \end{cases} \quad (14)$$

Where S_{max} and S_{min} are the maximum and minimum values of the battery charge respectively; $P_{c, max}$ and $P_{c, min}$ are the maximum and minimum values of the battery charging power, respectively; $P_{d, max}$ and $P_{d, min}$ are the maximum and minimum discharge power of the battery, respectively.

(3) Photovoltaic and wind turbine installation quantity constraints

$$\begin{cases} N_{PV, min} \leq N_{PV} \leq N_{PV, max} \\ N_{WT, min} \leq N_{WT} \leq N_{WT, max} \\ N_{BS, min} \leq N_{BS} \leq N_{BS, max} \end{cases} \quad (15)$$

Where $N_{PV, min}$, $N_{WT, min}$ and $N_{BS, min}$ are the minimum number of PV panels, WTGs, and batteries to be installed; $N_{PV, max}$, $N_{WT, max}$

and $N_{BS,max}$ are the maximum number of PV panels, WTGs, and batteries to be installed according to the actual site.

3 Microgrid capacity optimization algorithm for green storage

3.1 Sparrow search algorithm (SSA)

The sparrow search algorithm (SSA) originates from observing the survival behavioral patterns of a sparrow population, which contains discoverers, early warners, and followers. The discoverer searches for food while guiding the follower to access resources, and the less adapted sparrows forage around and even compete for the discoverer's food, but the population share of both remains stable in the competition. Marginal individuals tended to move to relatively safe positions, while central individuals reduced the risk of predation. Alerts are issued when predators are detected, and when warnings exceed a safety threshold, the discoverer leads the follower to move toward a safe area. This algorithm can be applied to solve a variety of optimization problems by modeling the collaborative, competitive, and adaptive behavior of groups of organisms.

Discoverer location update strategy is:

$$X_{i,j}^{t+1} = \begin{cases} X_{i,j}^t \cdot \exp\left(-\frac{i}{\beta \cdot iter_{max}}\right), if R_2 < ST \\ X_{i,j}^t + Q \cdot L, if R_2 \geq ST \end{cases} \quad (16)$$

Where $X_{i,j}^t$ is the value of j ($j = 1, 2, 3, \dots, D$) dimension of the i ($i = 1, 2, 3, \dots, n$) sparrow in the t iteration; β is a random number between (0,1); ST is a random number between [0.5,1]; $iter_{max}$ is the maximum number of iterations; R_2 is a random number between [0,1]; Q is a random number that satisfies the normal distribution; L denotes a D dimensional vector with elements of one in each dimension.

The formula for updating the position of the followers is as follows:

$$X_{i,j}^{t+1} = \begin{cases} Q \cdot \exp\left(\frac{X_{worst}^t - X_{i,j}^t}{i^2}\right), i > n/2 \\ X_p^{t+1} + |X_{i,j}^{t+1} - X_p^{t+1}| \cdot A^+ \cdot L, others \end{cases} \quad (17)$$

Where X_p denotes the optimal position owned by the discoverer; X_{worst} denotes the global worst position; A denotes the matrix where the elements within the matrix will be randomly assigned a value of one or -1 to $1 \times d$, and $A^+ = A^T(AA^T)^{-1}$.

The updating formula for an early warning person's position is as follows:

$$x_{i,j}^{t+1} = \begin{cases} x_{best}^t + \beta \cdot |x_{i,j}^t - x_{best}^t|, f_i > f_g \\ x_{i,j}^t + K \cdot \left(\frac{|x_{i,j}^t - x_{worst}^t|}{f_i - f_w + \epsilon}\right), f_i = f_g \end{cases} \quad (18)$$

Where x_{best}^t denotes the current global optimal position; β is a standard normally distributed random number; K is a random

number in [-1,1]; f_i denotes the fitness value of the current individual sparrow; f_g is the fitness value of the global optimal position; f_w is the fitness value of the global worst position; the smallest parameter, ϵ , is used to avoid the denominator to be 0; when $f_i > f_g$, the sparrow is easy to be attacked by the natural enemy, and when $f_i = f_g$, the sparrow is aware of the danger to approach to other sparrows.

Although the SSA is superior to traditional heuristic algorithms such as particle swarm optimization (PSO) and grey wolf optimization (GWO) in terms of optimization ability and convergence speed, some solutions of SSA will gather near the origin in the later stage of iteration, which reduces the diversity of sparrow population and increases the possibility of 'premature' convergence. To deal with these problems, this paper proposes an improved sparrow search algorithm.

3.2 ISSA for optimal configuration of microgrid capacity for green storage

3.2.1 Chaos mapping strategy

To solve problems such as the lack of diversity of sparrow populations in later iterations, this paper introduces chaotic mapping to generate the initial sparrow populations to increase their diversity and improve the quality of the initial solution of the algorithm. The particle distribution scatter plot and histogram are shown in Figure 2. Chaotic variables are random, so in the search optimization problem, it is used to increase the population diversity of the algorithm and improve the ability of the algorithm to jump out of the local optimal solution, thereby enhancing the global search performance of the algorithm.

Gao (2021) created a Logistic-Tent composite chaotic system by combining the classical one-dimensional Logistic chaotic system and the Tent chaotic system. This chaotic system combines the complex chaotic dynamics of the Logistic system with a faster iteration speed, more autocorrelation, and applicability to a large number of sequences of the Tent system, which is defined by the following mathematical formula:

$$X_{n+1} = \begin{cases} (rX_n(1 - X_n) + (4 - r)X_n/2) \bmod 1, X_n < 0.5 \\ (rX_n(1 - X_n) + (4 - r)(1 - X_n)/2) \bmod 1, X_n \geq 0.5 \end{cases} \quad (19)$$

Where X_n is the system variable, $X_n \in [0, 1]$; r is the control parameter, $r \in (0, 4)$, in this paper, $r = 0.1$.

3.2.2 Adaptive t-distribution variation strategy

Because the t-distribution combines the robustness of the Cauchy-distribution and the smoothness of the Gaussian-distribution, the adaptive t-distribution variation strategy for the leading discoverers in the population can allow the discoverers to search for the best point faster. The adaptive t-distribution variation strategy aims to make the algorithm show strong global development ability in the early stage of iteration, and show good local exploration ability in the later stage of iteration, and improve the convergence speed of the algorithm. In this way, the advantages of global search and local search can be comprehensively utilized throughout the iteration process to optimize the SSA more

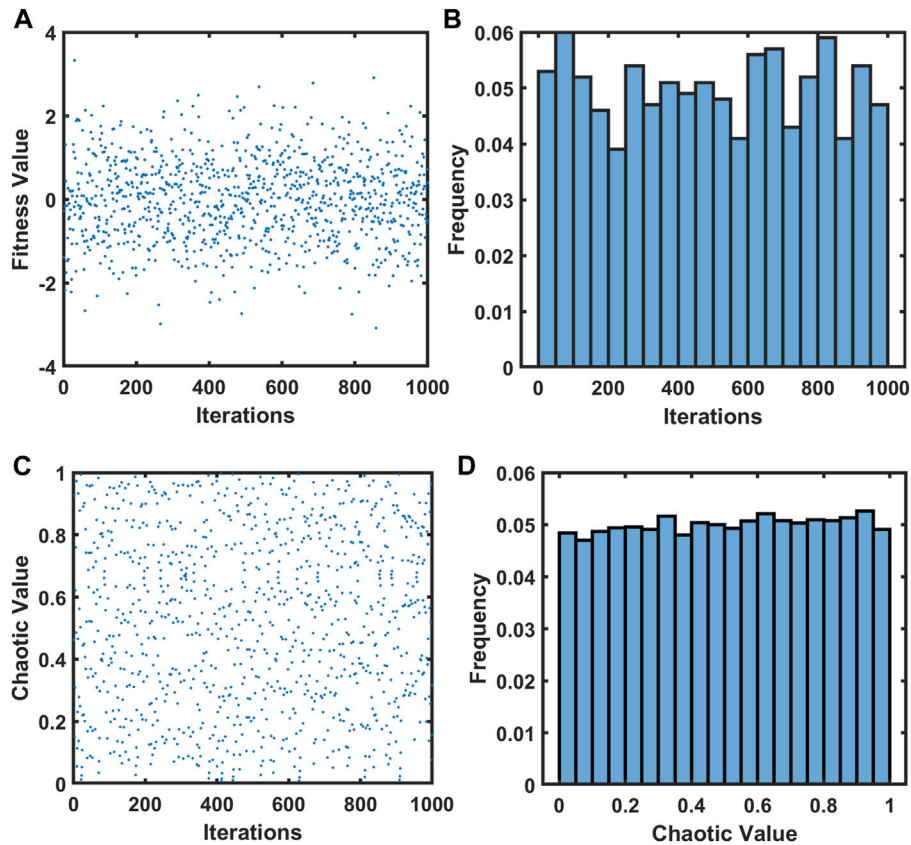


FIGURE 2 Comparison of scatter plot and histogram of particle distribution. (A) SSA Initial Particle Distribution Plot. (B) SSA Initial Particle Distribution Histogram. (C) Chaos Algorithm Initial Particle Distribution Plot. (D) Chaos Algorithm Initial Particle Distribution Histogram.

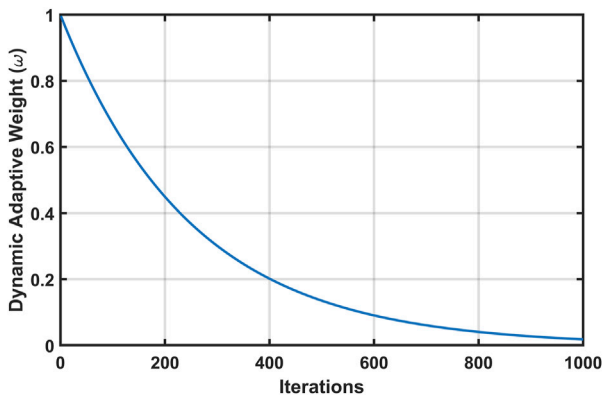


FIGURE 3 Dynamic adaptive weight change curve.

effectively. The improved discoverer’s location update method is as follows:

$$X_{new} = X_{i,j}^{t+1} + \omega \cdot X_{i,j}^{t+1} \cdot t(iter) \tag{20}$$

$$X_{i,j}^{t+1} = \begin{cases} X_{new}, & f_i < f_t \\ X_{i,j}^{t+1}, & \text{others} \end{cases} \tag{21}$$

Where $X_{i,j}^{t+1}$ is the value of the $j(j = 1, 2, 3, \dots, D)$ dimension of the $i(i = 1, 2, 3, \dots, n)$ sparrow in the $t + 1$ iteration; $t(iter)$ is the t -distribution of $iter$ for the parameter degrees of freedom, and with the increase of the number of iterations $iter$, the t -distribution gradually converges to the Gaussian distribution, which is conducive to the enhancement of the convergence speed of the algorithm; ω is the adaptive parameter. X_{new} is the position of the sparrow after variation disturbance; f_i is the individual fitness value of the i discoverer; f_t is the average fitness value of the discoverer; if $f_i < f_t$, the t -distribution mutation perturbation is performed, otherwise the mutation perturbation will not be performed.

The purpose of introducing the adaptive parameter ω is to increase the population diversity in the early stage of the algorithm while ensuring that the optimal solution for the sparrow population can be retained in the later stage. The change curve of adaptive parameters is shown in Figure 3. At the initial stage of iteration, the adaptive parameter ω can take a larger value to increase the population diversity through the new solution generated by the t -distribution variation. As the number of iterations increases and the algorithm approaches the optimal solution, the role of the adaptive parameter ω is gradually reduced to ensure that the optimal solution in the sparrow population is fully retained. This strategy balances the need for global exploration and local optimization during the search process. The formula for calculating the adaptive parameter is as follows:

Algorithm 1 Improved sparrow search algorithm

Input: population_size, max_iterations, dimension, PD, SD, ST, lower_bound, upper_bound.

Output: global_best_position.

```

1 Procedure:
2   % Initialize parameters
3   population_size, max_iterations, dimension, PD, SD, ST, lower_bound, upper_bound.
   -Parameters
4   % Initialize population using Logistic-Tent chaotic map
5   population = Initialize_Population(population_size, dimension, lower_bound, upper_bound)
6   for iter from 1 to max_iterations:
7     Evaluate fitness value for each sparrow in population
8     Sort population based on fitness values
9     best_fitness = fitness value of the best sparrow
10    best_position = position of the best sparrow
11    for each discoverer in population:
12      if discoverer's fitness > average fitness of population:
13        Update discoverer position using Formula (16)
14      else:
15        Update discoverer position using Formula (20) and Formula (21)
16    for each follower in population:
17      Update follower position using Formula (17)
18    for each alerter in population:
19      Update alerter position using Formula (18), Formula (23) and Formula (24)
20    if max_iterations reached or termination condition met:
21      Output global_best_position

```

FIGURE 4
Pseudo-code of ISSA.

$$\omega = \omega_{\text{start}} \cdot \exp\left(-\frac{t}{\alpha}\right) \quad (22)$$

Where ω_{start} is the initial value of the decrement; t is the current iteration number; α is the parameter to control the decrement speed, in this paper, $\alpha = 250$.

3.2.3 Mixed decreasing strategy

In the SSA, the step control parameters K and β of the vigilant play a key role in balancing the global search and local search, and the search efficiency and accuracy of the algorithm can be improved by adjusting its parameters. For this reason, this paper uses a hybrid decreasing strategy to adjust this parameter.

This strategy can dynamically adjust the search strategy according to the changes in the number of iterations, gradually shifting from a global search to a more focused local search, and the mathematical representation of this strategy is shown in the following Equation. With this strategy, the behavior of the algorithm can be flexibly adjusted at different stages to better adapt to the complexity of the problem and the characteristics of the search space.

$$K = \frac{1}{2} (K_{\text{max}} - K_{\text{min}}) \left(1 + \cos \frac{\pi n}{N_{\text{max}}} \right) + K_{\text{max}} \quad (23)$$

Where K is the current value of the vigilant parameter; K_{max} is the maximum value, representing the maximum search capability of the vigilant; K_{min} is the minimum value, representing the minimum search capability of the vigilant; n is the current number of iterations; N_{max} is the maximum number of iterations.

The step control parameter β adopts a linear decreasing strategy, that is, decreasing its value at a fixed step size in each iteration, as shown in the following formula.

$$\beta = \beta_{\text{max}} - \frac{n}{N_{\text{max}}} (\beta_{\text{max}} - \beta_{\text{min}}) \quad (24)$$

Where β_{max} and β_{min} are the maximum and minimum values of, respectively.

The hybrid decrementing strategy cleverly combines two different decrementing methods to adapt the search behavior of the algorithm more flexibly and efficiently. Such a strategy makes it possible to find an appropriate balance between global and local search, ensuring a better adaptation to the nature of the problem at different stages of the algorithm, thus improving the efficiency and accuracy of the search.

Based on the proposed improvement strategy, the pseudo-code of the ISSA is shown in Figure 4, and the process of solving the capacity optimization configuration of the ISSA is shown in Figure 5.

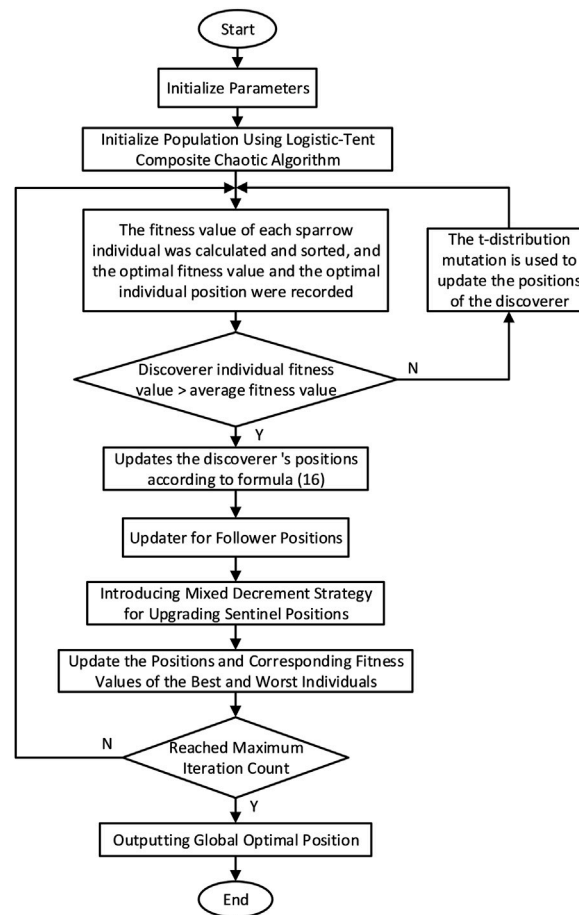


FIGURE 5
Flow chart of ISSA.

Step 1: Initialization parameters: the population size is n , the maximum number of iterations is is , the spatial dimension is J , the number of discoverers is PD , the number of alerts is SD , the alarm threshold is ST , the initial upper and lower bounds are lb and ub , and the fitness function is;

Step 2: Population initialization: generate the initial population according to Eq. 19;

Step 3: Calculates and sorts the fitness value of each sparrow individual, and records the optimal fitness value and the optimal individual position;

Step 4: Determines whether the individual fitness value of the discoverer is greater than the average fitness value. If it is greater than, the location of the discoverer is updated according to Eq. 16. If the conditions are not met, the location of the discoverer is updated according to Eqs 20–22;

Step 5: Update the follower position according to Eq. 17;

Step 6: Update the follower position according to Eqs 18–24;

Step 7: Update the position of the best and worst individuals and the corresponding fitness value;

Step 8: Until the maximum number of iterations is reached, the global optimal position is output.

In summary, the SSA itself has a certain global search ability. Introducing the Logistic-Tent chaos mapping strategy and the adaptive t-distribution variation strategy, can not only further

enhance the global search ability of the algorithm, but also help the algorithm to perform more effectively in the search process. These two strategies help to explore potential optimization solutions more extensively in the search space and fine-tune the performance of solutions. The mixed decreasing strategy is introduced to the step size control parameters of the early warning, and the decreasing step size strategy makes the algorithm less sensitive to the choice of initial parameters. Even if the initial parameter setting is not good, the algorithm still can achieve good optimization results by gradually adjusting the step size in the later stage, which enhances the robustness of the algorithm. Therefore, the ISSA can improve the search efficiency of the algorithm, avoid premature convergence, and enhance the robustness of the algorithm, which is helpful for better application to solve the problem of optimal capacity allocation of wind-solar-storage microgrid.

4 Case study

4.1 Date settings

Taking the storage in a certain area as an example object, according to the proposed capacity optimization allocation model and

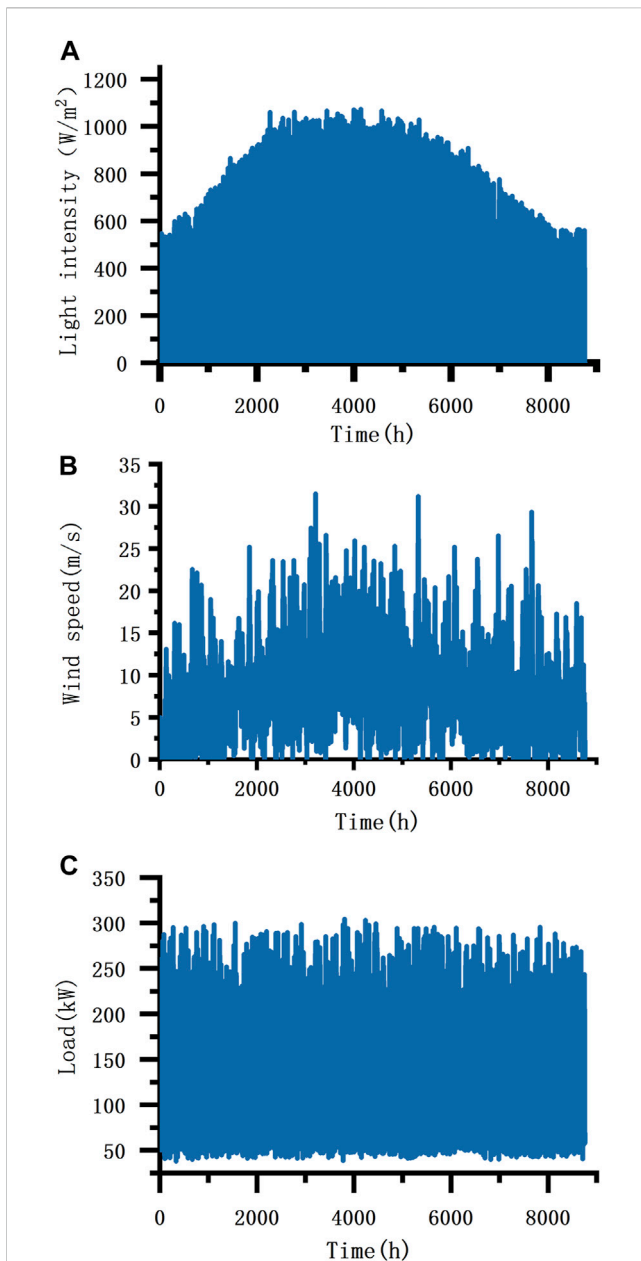


FIGURE 6 Annual data for this storage. (A) Hourly light intensity throughout the year. (B) Hourly wind speed throughout the year. (C) Hourly loads throughout the year.

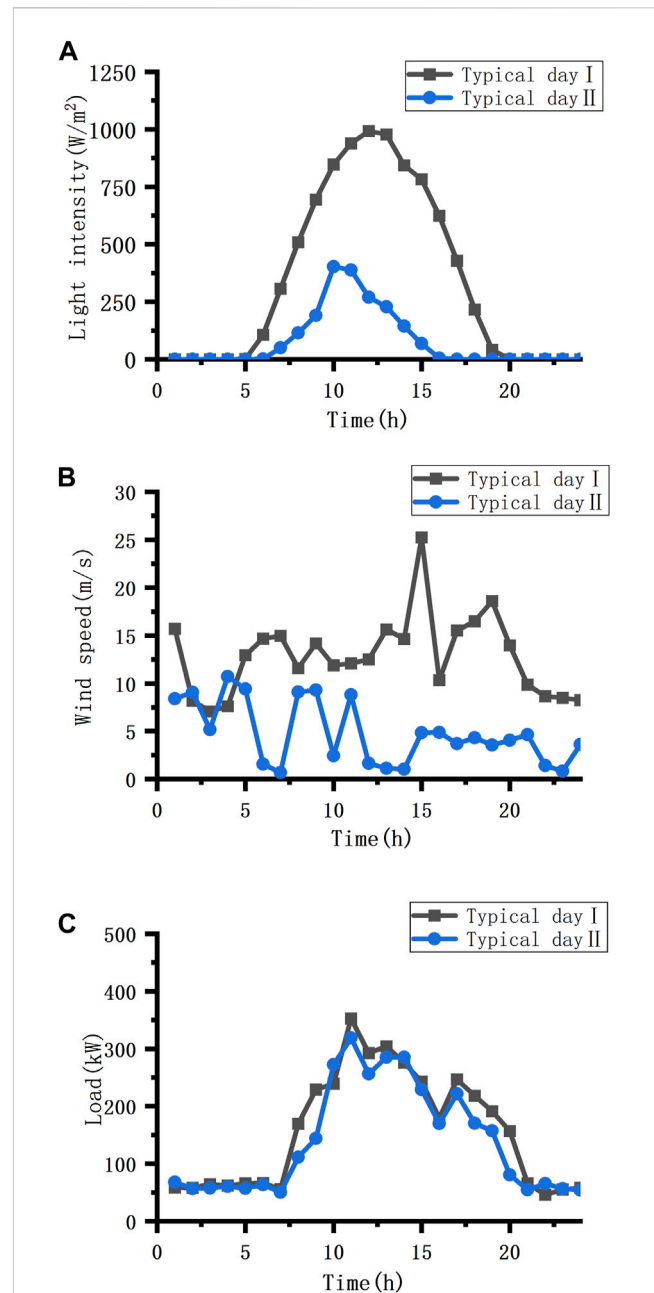


FIGURE 7 Weather conditions and load demand under two typical days. (A) Light intensity. (B) Wind speed. (C) Load demand.

TABLE 1 Distributed power economy parameters.

Equipment	Capacity (kW)	Investment cost coefficient (yuan/kW)	Annual operation and maintenance costs (yuan/kW)	Replacement cost (yuan/kW)	Lifespan (a)
WTG	35	4237	36.2	—	20
Solar panel	25	3550	50.3	—	25
Battery unit	30	450	137.7	500	10

optimization strategy, the ISSA is used to optimize the capacity of the wind-solar-storage system in a microgrid. The total electricity consumption of the storage load for the whole year (8760 h) is

1.004 MWh, and the average load is 114.59 kWh, while the average annual wind speed of the region is 8.43 m/s, and the average light intensity is 234W/m², and the data of the storage is shown in [Figure 6](#).

TABLE 2 Time-share electricity purchase and sale tariffs.

Time-of-use intervals	Times	Purchased electricity (yuan/kWh)	Electricity sales (yuan/kWh)
Peak	7:00-11:00, 17:00-21:00	0.588	0.501
Off-peak	23:00-7:00 the following day	0.328	0.27
Shoulder	11:00-17:00, 21:00-23:00	0.538	0.45

TABLE 3 Capacity allocation results.

Configuration		Application scenes	
		Typical day I	Typical day II
Number of equipment	WTGs	2	3
	Solar panels	10	13
	Battery units	3	5
Payback period (years)		9	11
Investment cost (million yuan)		122.46	166.61
Maintenance Cost (million yuan)		2.75	4.08
Wind and Solar Utilization Rate		89%	89%
Self-Balancing Rate		94.46%	51.89%

To capture the performance characteristics of the system under seasonal extreme conditions, the performance characteristics of the system under high wind speed, low wind speed, high light intensity, and low light intensity are considered, and two typical days are selected and their data are analyzed; the typical days are July in summer when the wind speed is high and the light intensity is high, and December in winter when the wind speed is low and the light intensity is low, as shown in Figure 7. The economic parameters of the configured wind-solar storage equipment are shown in Table 1. The electricity price between the microgrid system and the power grid in different periods is shown in Table 2.

In Figure 7, the light intensity of typical day I was larger from 10:00 to 15:00, and there was no light at about 19:00, and the wind

speed was larger in the whole period. On the typical day II, the light intensity was larger during the period of 10:00–12:00, and there was no light at 17:00. The wind speed was larger during 1:00–5:00 and 8:00–11:00.

4.2 Microgrid capacity configuration results in green storage

To verify the optimal configuration model of power capacity of a wind-solar-storage microgrid in this paper, simulation analysis is carried out in two typical days. The capacity configuration results of the wind-solar-storage microgrid for green storage are in Table 3. The operation of the two typical days under the optimal capacity configuration results is shown in Figure 8.

Table 3 shows that the investment cost of typical day I is less than that of typical day II, the payback period is also shorter than that of typical day II, and the number of PV panels and wind turbines connected is less than that of typical day II. This shows that the economy of the system is superior under the climate conditions of typical day I. Under different climate conditions, the number of PV panels and wind turbines need to be adjusted to ensure that the system can operate efficiently under various weather conditions and to improve the overall economy, and better climate conditions make the system require less investment in equipment under the condition of obtaining the same amount of power generation. Such a comparison illustrates that the wind and solar storage capacity configuration must take full account of local climatic conditions and that different wind and solar weather will directly affect the capacity configuration of the system, and thus the economics. Under better wind and solar

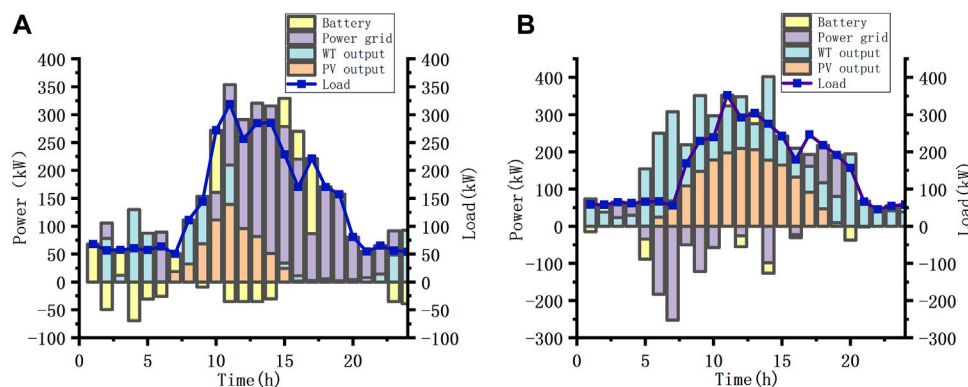


FIGURE 8 The operation of two typical days under the optimal capacity configuration results (A) Operation of typical day I. (B) Operation of typical day II.

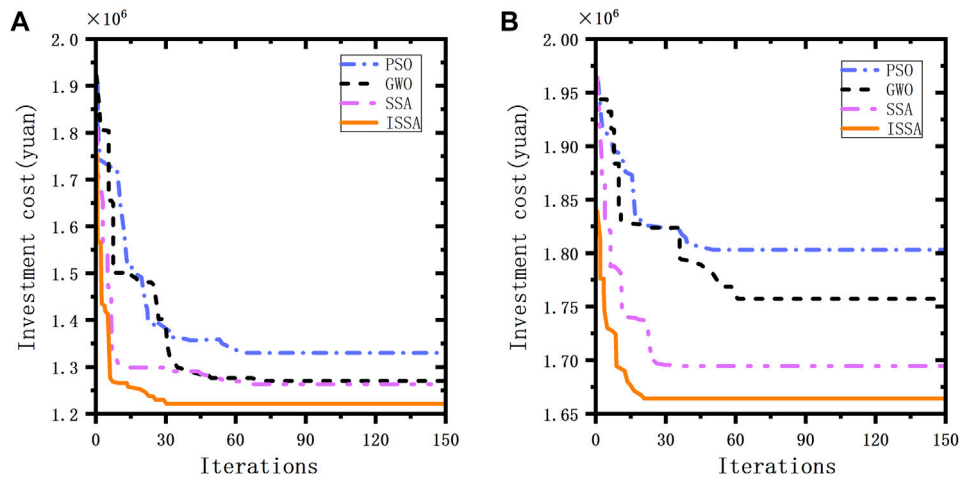


FIGURE 9 Comparison of iterative optimization curves of four optimization algorithms (A) Comparison of iterative optimization curves of typical day I. (B) Comparison of iterative optimization curves of typical day II.

TABLE 4 Algorithm parameter settings.

Algorithms	Parameter setting
ISSA	$PD = 0.2 * n, SD = 0.2 * n, ST = 0.8, r = 0.1, \alpha = 250$
SSA	$PD = 0.2 * n, SD = 0.2 * n, ST = 0.8$
PSO	$\omega_{max} = 0.8, \omega_{min} = 0.2, c_1 = c_2 = 2.5$
GWO	$a \in [0, 2], b = 1.5, p$ is a random number of $[0, 1]$

TABLE 5 Comparison of capacity configuration results of four algorithms.

Algorithms	Investment cost (million yuan)	
	Typical day I	Typical day II
ISSA	122.46	166.61
SSA	125.35	171.54
PSO	134.29	182.18
GWO	127.55	174.62

climatic conditions, the system is more likely to obtain higher power generation efficiencies, which reduces the need for equipment, lowers the cost of investment, and shortens the payback period.

The wind and light utilization rates of typical day I and typical day II are both higher, indicating that the system can convert solar and wind energy into electricity more efficiently and maximize the use of renewable resources, which is of great significance for improving the economy and sustainability of the system. In Figure 9, there is no need to purchase electricity from the power grid on the typical day I from 8:00 to 16:00 during the peak period of electricity consumption, and electricity can be sold to the power grid from 7:00 to 10:00 and 11:00 to 13:00. The self-balancing rate of the system is high, which reduces the

dependence on the external power grid, increases the independence of the system, and improves the comprehensive utilization rate of the system energy. In contrast, the self-balancing rate of typical day II is low, and power is purchased from the power grid from 10:00 to 19:00 during the peak period of power consumption, indicating that the system is more dependent on the external power grid to meet the power demand, thus increasing the operating cost and reducing the self-sufficiency of the system.

4.3 Comparison of algorithms

In this paper, ISSA, SSA, PSO and GWO are used to analyze the investment cost of the two typical days of the wind-solar-storage model. The algorithm parameters are set as shown in Table 4, the population size is uniformly set to 100, and the number of iterations is uniformly set to 150. The simulation experiment is run under the Matlab 2023a simulation platform. The comparison of the four algorithms is shown in Table 5, and the iterative optimization curve is shown in Figure 9.

It can be seen from Table 5 that the ISSA algorithm has achieved the minimum investment cost in two different typical days. Compared with the other three algorithms (SSA, PSO and GWO), ISSA decreased by 2.36%, 9.66% and 4.16% on typical day I, and decreased by 2.96%, 9.34% and 4.81% on typical day II, respectively. This shows that the ISSA algorithm has a lower cost than other algorithms in the wind-solar-storage investment cost allocation model. Further analysis of Figure 9 shows that the ISSA adopts the Logistic-Tent composite chaotic mapping strategy, which makes it have a faster convergence speed at the initial stage of iteration. In contrast, the other three algorithms (SSA, GWO, PSO) fall into the local optimal solution. This shows that the ISSA has better global search ability in optimizing the objective function, and can more effectively avoid falling into the local optimal solution. The improvement of this global search ability makes the ISSA algorithm better find the optimal solution for investment cost.

In summary, ISSA not only achieves better results in the cost allocation model of wind-solar-energy storage investment but also shows faster convergence speed and better global search ability in the optimization process.

5 Conclusion

In this paper, aiming at the premature convergence of SSA to local optimal solution in the later stage of iteration, ISSA is adopted, including three improved strategies: Logistic-Tent composite chaotic map, adaptive t-distribution mutation and mixed decreasing. Compared with the standard SSA, PSO and WGO, ISSA not only achieves better results in the configuration model but also shows faster convergence speed and better global search ability in the optimization process. It is proved that ISSA effectively improves the global optimization performance of the algorithm. Based on the establishment of the microgrid capacity configuration model for green storage, the shortest payback period is proposed as the objective function, and the influence of time-of-use electricity price and different weather conditions on the system is fully considered. For the problem of optimal configuration of microgrid capacity for green storage, ISSA provides an important reference value for the optimal configuration of the model.

Data availability statement

The original contributions presented in the study are included in the article/Supplementary material, further inquiries can be directed to the corresponding author.

Author contributions

NZ: Conceptualization, Funding acquisition, Supervision, Writing–original draft, Writing–review and editing. XM:

Conceptualization, Methodology, Writing–original draft, Writing–review and editing. ZG: Investigation, Project administration, Writing–review and editing. CS: Data curation, Validation, Visualization, Writing–review and editing. JL: Conceptualization, Data curation, Writing–review and editing.

Funding

The author(s) declare that financial support was received for the research, authorship, and/or publication of this article. This work was financially supported by the State Grid Liaoning Electric Power Co, Ltd. Science and Technology Project (2023YF-160).

Conflict of interest

Authors NZ, XM, ZG, and CS were employed by State Grid Liaoning Electric Power Supply Co., Ltd. Branch Materials. Authors NZ, XM, ZG, and CS were employed by State Grid Corporation of China.

The remaining author declares that the research was conducted in the absence of any commercial or financial relationships that could be construed as a potential conflict of interest.

The authors declare that this study received funding from State Grid Liaoning Electric Power Co, Ltd. The funder had the following involvement in the study: Supervision, Conceptualization, Methodology, Investigation, Date curation, Validation, Visualization.

Publisher's note

All claims expressed in this article are solely those of the authors and do not necessarily represent those of their affiliated organizations, or those of the publisher, the editors and the reviewers. Any product that may be evaluated in this article, or claim that may be made by its manufacturer, is not guaranteed or endorsed by the publisher.

References

- Borhanazad, H., Mekhilef, S., Ganapathy, V. G., Modiri-Delshad, M., and Mirtaheri, A. (2014). Optimization of micro-grid system using MOPSO. *Renew. energy* 71, 295–306. doi:10.1016/j.renene.2014.05.006
- Chen, C., Wang, Y., Xie, X., Wang, J., and Xiao, B. (2023b). Improved chaotic seagull optimisation algorithm incorporating sparrow search mechanism. *Sci. Technol. Eng.* 23 (10), 4259–4271.
- Chen, R. (2023a). *Two-layer optimization of power capacity in microgrid considering demand response*. Guangxi: Guangxi University. master's thesis. doi:10.27034/d.cnki.ggxu.2023.000765
- Diaf, S., Diaf, D., Belhamel, M., Haddadi, M., and Louche, A. (2007). A methodology for optimal sizing of autonomous hybrid PV/wind system. *Energy policy* 35 (11), 5708–5718. doi:10.1016/j.enpol.2007.06.020
- Duláu, L.-I. (2023). Power cost and CO2 emissions for a microgrid with hydrogen storage and electric vehicles. *Sustainability* 15, 15750. doi:10.3390/su152215750
- Gao, J., Yan, W., Pau, G., Lin, L., and Wen, Y. (2023). Multi-objective capacity optimization configuration of independent wind-photovoltaic-hydrogen-battery system based on improved MOSSA algorithm. *Front. Energy Res.* 10, 1077462. doi:10.3389/fenrg.2022.1077462
- Gao, Y. (2021). *Pseudo-random sequence IP design based on logistic chaos algorithm*. Heilongjiang: Heilongjiang University. master's thesis. doi:10.27123/d.cnki.ghlju.2021.000474
- Guo, Y., Zhang, J., He, Y., Liu, Y., Deng, K., and Long, B. (2022). Hybrid energy storage configuration of micro-grid considering charge-discharge response of EVs. *Power Grid Clean Energy* 38 (08), 82–93.
- Jiang, J., Fu, S., Qi, X., Zhang, X., and Wang, D. (2023a). Research on energy storage capacity optimization and operation control strategy of wind-solar-storage system in the park. *Electr. Technol. And Econ.* 10, 110–112.
- Jiang, X. (2021). Research on the development path and countermeasures of green logistics in China. *Logist. Eng. Manag.* 11, 16–18.
- Jiang, Z., Xiang, Y., Tan, Z., Guo, Y., Wang, Y., and Zhou, K. (2023b). Optimal configuration of energy storage capacity in high-proportion clean energy parks considering demand response. *China Electr.* 56 (12), 147–155+163.
- Justus, C. G. (1978). Wind energy statistics for large arrays of wind turbines (New England and Central US Regions). *Sol. Energy* 20 (5), 379–386. doi:10.1016/0038-092x(78)90153-6
- Kumar, N., Singh, B., and Panigrahi, B. K. (2019). Grid synchronisation framework for partially shaded solar PV-based microgrid using intelligent control strategy. *IET Generation, Transm. Distribution* 13 (6), 829–837. doi:10.1049/iet-gtd.2018.6079
- Kumar, N., Singh, B., Wang, J., and Panigrahi, B. K. (2020). A framework of L-HC and AM-MKF for accurate harmonic supportive control schemes. *Circuits Syst. I Regul. Pap. IEEE Trans.* 67 (99), 5246–5256. doi:10.1109/tcsi.2020.2996775

- Lazaroiu, A. C., Gmal Osman, M., Strejoiu, C.-V., and Lazaroiu, G. (2023). A comprehensive overview of photovoltaic technologies and their efficiency for climate neutrality. *Sustainability* 15, 16297. doi:10.3390/su152316297
- Lei, W., Jun, P., Wei, J., and Yu, L. (2024). Bi-level optimization configuration method for microgrids considering carbon trading and demand response. *Front. Energy Res.* 11, 1334889. doi:10.3389/fenrg.2023.1334889
- Li, Q., and Hu, R. (2023). Analysis of the development status of green logistics under the background of double carbon. *Logist. Eng. And Manag.* 45 (06), 1–3.
- Li, R., and Zhang, W. (2016). Energy demand forecasting of logistics industry based on RBF neural network. *Resour. Sci.* 38 (03), 450–460.
- Lin, L. (2021). *Research on multi-objective optimal scheduling and shared energy storage capacity allocation of micro-energy networks based on typical scenarios*. Zhejiang: Zhejiang University. master's thesis.
- Liu, S. (2023). The planning scheme of the development path of the logistics park under the background of double carbon is constructed. *Time-honored Brand Mark.* (24), 44–46.
- Lv, X., Mu, X., Zhang, J., and Wang, Z. (2021). Chaotic sparrow search optimisation algorithm. *J. Beijing Univ. Aeronautics Astronautics* 47 (08), 1712–1720. doi:10.13700/j.bh.1001-5965.2020.0298
- Ma, G. (2023). Low-carbon economy promotes the transformation and upgrading of logistics industry. *Public Invest. Guide* 13, 191–193.
- Nan, B., Dong, S., Tang, K., Zhu, M., Zhang, X., and Chen, W. (2023). Optimal configuration of energy storage in PV-storage microgrid considering demand response and uncertainties in source and load. *Power Grid Technol.* 47 (04), 1340–1352. doi:10.13335/j.1000-3673.pst.2022.0798
- Saxena, V., Kumar, N., Singh, B., and Panigrahi, B. K. (2021). An MPC based algorithm for a multipurpose grid integrated solar PV system with enhanced power quality and PCC voltage assist. *IEEE Trans. Energy Convers.* 36 (2), 1469–1478. doi:10.1109/tec.2021.3059754
- Su, W., Zheng, W., Li, Q., Yu, Z., Han, Y., and Bai, Z. (2023). Capacity configuration optimization for green hydrogen generation driven by solar-wind hybrid power based on comprehensive performance criteria. *Front. Energy Res.* 11, 1256463. doi:10.3389/fenrg.2023.1256463
- Wang, J., Miao, S., Yao, F., Wang, Y., Lin, S., and Wei, W. (2023). Multi-objective capacity optimization configuration in microgrid considering life cycle carbon metering and carbon trading mechanism. *Mod. Electr.*, 1–10.
- Wang, X., Chen, Z., Bian, Z., Wang, Y., and Wu, Y. (2022). Optimal allocation of a wind–PV–battery hybrid system in smart microgrid based on particle swarm optimization algorithm. *Integr. Smart Energy* 44 (06), 52–58.
- Wang, Y., and Chen, J. (2023). Optimal allocation of hybrid energy storage capacity for optical storage microgrid based on ISSA. *Intell. Power* 51 (04), 23–29+53.
- Wu, M. (2023). *Capacity optimization configuration model for Wind-Photovoltaic power generation coupled with hydrogen energy storage system under carbon emission reduction*. Beijing: North China Electric Power University. master's thesis. doi:10.27140/d.cnki.ghbbu.2023.001113
- Xiong, X., Hu, X., and Guo, H. (2021). A hybrid optimized grey seasonal variation index model improved by whale optimization algorithm for forecasting the residential electricity consumption. *Energy* 234, 121127. doi:10.1016/j.energy.2021.121127
- Xu, Y., and Hu, Z. (2024). Source-grid-load cross-area coordinated optimization model based on IGDT and wind-photovoltaic-photothermal system. *Sustainability* 16, 2056. doi:10.3390/su16052056
- Xu, Z., Chen, F., Yang, X., and Lu, Q. (2024). Optimal configuration of hybrid energy storage capacity in a grid-connected microgrid considering laddering carbon trading and demand response. *Energies* 17, 139. doi:10.3390/en17010139
- Yan, Q., Jia, Y., Ma, Y., and Song, X. (2024). Two-layer energy management strategy of microgrid based on Stackelberg master-slave game. *J. Sol. Energy*, 1–9.
- Yang, X. (2010). A new meta-heuristic bat-inspired algorithm. *Nat. Inspired Coop. Strategies Optimization*, 66–73.
- Yang, X., Zi, C., Han, W., and Yang, Y. (2023). A review of green warehousing research. *Environ. Prot. Circular Econ.* 43 (09), 4–6+94.
- You, B. (2024). Research on green development strategy of logistics enterprises in low carbon economy environment. *Mall. Mod.* (01), 21–23. doi:10.14013/j.cnki.scxdh.2024.01.001
- Zhang, P., Lu, X., and Meng, Q. (2023). Optimal allocation of microgrid capacity based on multi-strategy sparrow search algorithm. *Electr. Technol.* 24 (01), 1–9.
- Zhao, C., Wang, B., Sun, Z., and Wang, B. (2022). Optimal configuration of independent microgrid capacity based on improved grey wolf algorithm. *J. Sol. Energy* 43 (01), 256–262. doi:10.19912/j.0254-0096.tynxb.2020-0042